Atomic Force Microscopy Imaging of DNA under Macromolecular Crowding Conditions

David Pastré,*,† Loïc Hamon,† Alain Mechulam,† Isabelle Sorel,† Sonia Baconnais,‡,§ Patrick A. Curmi,† Eric Le Cam,‡,§ and Olivier Piétrement‡,§

Laboratoire Structure et Activité des Biomolécules Normales et Pathologiques, INSERM U829/Université d'Evry EA3637, Rue du Père Jarlan, 91025 Evry Cedex, France, CNRS, Laboratoire de Microscopie Moléculaire et Cellulaire, UMR 8126 Interactions Moléculaires et Cancer, Institut de cancérologie Gustave Roussy, Villejuif, F-94805, France, and Université Paris Sud, Villejuif, F-94805, France

Received May 11, 2007

Studying the influence of macromolecular crowding at high ionic strengths on assemblies of biomolecules is of particular interest because these are standard intracellular conditions. However, up to now, no techniques offer the possibility of studying the effect of molecular crowding at the single molecule scale and at high resolution. We present a method to observe double-strand DNA under macromolecular crowding conditions on a flat mica surface by atomic force microscope. By using high concentrations of monovalent salt ([NaCl] > 100 mM), we promote DNA adsorption onto $NiCl_2$ pretreated muscovite mica. It therefore allows analysis of DNA conformational changes and DNA compaction induced by polyethylene glycol (PEG), a neutral crowding agent, at physiological concentrations of monovalent salt.

Introduction

In the cell, DNA evolves and functions with a monovalent ion concentration of about 150 mM and in a crowded space[1–6] where the concentration of macromolecules (e.g., proteins, nucleic acids, or complex sugars) can reach 400 mg/mL.[7] Monovalent ions are essential to many aspects of cellular function as they favor specific interactions among biomolecules and decrease nonspecific binding in particular for DNA−ligand recognition.[8,9] Molecular crowding has also several important effects on the DNA−ligand interactions.[10,11] It induces DNA compaction[12] and considerably influences the DNA–protein interactions and kinetics.[13,14] Macromolecular crowding plays also a critical role for several processes such as DNA replication or transcription.[15] This is why several groups have already used optical microscopy to observe DNA compaction by molecular crowding.[12,16–18] The recent arrival of single-molecule techniques in this field is of major importance for a better understanding of biomolecular interactions at the single molecule level,[19] but the lateral resolution is not satisfactory to observe conformational changes (>200 nm). For this reason we propose to use an atomic force microscope since its lateral resolution is 2 orders of magnitude better (<1 nm) and no fluorescent tags are required. Transmission electron microscopy (TEM) has also been used for this purpose,[20–22] and TEM images of isolated nucleoids[23] and nucleosome core particles[24] compacted by macromolecular crowding are already reported. Surprisingly, despite the growing interests in using AFM to investigate DNA conformations and DNA−protein interactions, the AFM potential has not yet been exploited to perform these studies under excluded volume conditions, most probably because no method was available to observe DNA under such conditions by AFM. In this paper, we develop a simple method to adsorb DNA molecules on mica under macromolecular crowding conditions and at high monovalent salt concentrations, which then allows one to observe DNA compaction at high resolution by AFM.

In the first section, we show both theoretically and experimentally that DNA adsorption on mica pretreated with a divalent transition metal cations (Ni^{2+}), which is generally used to reinforce DNA adsorption for AFM imaging in liquid,[25–28] is favored by increasing the monovalent salt concentration. The point is that it allows the observation of adsorbed DNA molecules by AFM in the absence of multivalent salt and in the presence of physiological concentrations of monovalent salt. These conditions are thus ideal to study DNA compaction by macromolecular crowding, which requires high ionic strength to weaken the electrostatic repulsion between the negatively charged DNA segments.

In the second section, we observe the DNA conformation under macromolecular crowding conditions using PEG (poly(ethylene glycol)) as neutral molecular crowding agent. DNA compaction is imaged in the presence of PEG of high molecular weight and at moderate and high ionic strengths, as expected from previous reports.[1–6]

Materials and Methods

DNA and Chemical Products. pBR322 plasmid and PEGs of various molecular weights were purchased from Sigma-Aldrich (Saint Quentin Fallavier, France): PEG 20K (MW∼16000–24000), PEG 4K (MW∼3500–4500), and PEG 1K (MW∼950–1050). Solutions were prepared by dissolving the crowding agent in buffer.

DNA fragments of 1440 bp were obtained from pBR322 plasmid (position 2576–4020) by PCR amplification. PCR product was the purified on an anion exchange miniQ column (Amersham Biosciences) with a SMART system (Amersham Biosciences), ethanol precipitated, and suspended in TE buffer (10 mM Tris, pH 7.5; 1 mM EDTA). The homogeneity in DNA length was controlled with gel electrophoresis and by TEM. Linearized pBR322 plasmids were obtained after digestion by EcoRV and were purified as described above.

* To whom correspondence should be addressed: tel, (33) 1 69 47 01 79; fax, (33) 1 47 69 01 65; e-mail, david.pastre@univ-evry.fr.

† Laboratoire Structure et Activité des Biomolécules Normales et Pathologiques, INSERM U829/Université d'Evry EA3637.

‡ CNRS, Laboratoire de Microscopie Moléculaire et Cellulaire, UMR 8126 Interactions Moléculaires et Cancer, Institut de cancérologie Gustave Roussy.

§ Université Paris Sud.

10.1021/bm700856u CCC: $37.00
Published on Web 11/19/2007

Mica Treatment. A 0.4 mL portion of 10 mM $NiCl_2$ solution was deposited onto one side of a freshly cleaved mica (muscovite) for 1 min. The mica was then thoroughly rinsed with pure water (18.2 MΩ cm resistivity, MilliQ, Millipore), dried with a filter paper to prevent the formation of salt crystals on the surface, and cut in pieces of 1 cm^2 area. Unless specified, DNA molecules were diluted to 2 μg/mL in 20 mM Tris-HCl pH 7.5 and different PEG and NaCl concentrations. Five microliters of the DNA solution was deposited onto the $NiCl_2$ pretreated mica for 1 min. The sample was then thoroughly rinsed with 0.02% uranyl acetate. Finally, the mica was dried with filter paper.

AFM Imaging. AFM imaging was carried out using a Nanoscope IIIa AFM (Veeco Instrument) in tapping mode with silicon cantilevers AC160TS (Olympus). The scan frequency was typically 1 Hz per line, and the modulation amplitude was approximately a few nanometers. All samples were imaged in air.

DNA Adsorption Mediated by Monovalent Salts on Pretreated Mica

The aim of this work was to develop a new method to adsorb DNA on mica compatible with both physiological ionic strength and molecular crowding environment. Although several substrates have been proposed to image DNA such as gold surface[29] or cationic lipid surface,[30] mica remains the most commonly used surface because of its flatness, facility to use, and performance in term of resolution.[31,32] DNA adsorption on mica is generally obtained via the addition of multivalent cations into the solution (Mg^{2+}, spermidine, . . .) either with bare or $NiCl_2$ pretreated mica surfaces.[26,32–34] Multivalent cations are generally used to generate an attraction force between DNA and mica, but their presence in solution is not satisfactory for studying DNA conformational changes under molecular crowding conditions. The problem is that DNA compaction can be triggered on the surface by the presence of divalent salt even with low concentrations of crowding agent (PEG).[19] In this context, silanized mica surfaces such as APTES−mica can be a good candidate for this study since the presence of multivalent cation in solution is not necessary for DNA adsorption. However adsorption of DNA to silanized mica also led to DNA adsorption condensation due to the presence of mobile cationic silanes on the surface, as previously reported.[35] Very few studies explored the possibility to image DNA in the presence of monovalent ions and in absence of divalent cations in solution. A work by Ellis et al.[36] presented evidence for DNA immobilization on bare mica in a liquid cell in the presence of about 14 mM NaCl, but we found that the binding in these conditions was too weak.[34,37] Instead, we used a $NiCl_2$ pretreated mica in order to generate an attraction mediated by the strongly adsorbed Ni^{2+} ions. In order to understand the mechanism of DNA adsorption on $NiCl_2$ pretreated mica in the absence of multivalent cations in solution, one has to consider the origin of the entropic repulsion, which prevents the DNA electrostatic adsorption on mica. Then we shall decipher what is the origin of the attraction force between DNA and mica mediated by the strongly adsorbed Ni^{2+} ions.

(1) The Entropic Repulsion Is Reduced at High Ionic Strength. As both DNA and mica are highly negatively charged surfaces, DNA and mica counterions tend to form a dense cloud on these surfaces (Figure 1A). The decay in the counterion concentrations within a distance d from a charged surface is[38]

$$n(d) = \frac{\mathrm{ns}}{(1 + d/2\lambda)^2} \quad (1)$$

$$\lambda = e/4\pi\sigma l_B \quad \text{and} \quad \mathrm{ns} = 2\pi(\sigma/e)^2 l_B \quad (2)$$

where ns is the surface concentration of the monovalent counterions, l_B is the Bjerrum length (0.7 nm), σ is the surface charge density, and λ is the Gouy–Chapman length. ns is about 6 M and λ about 0.12 nm for DNA. For bare mica, ns is around 26 M, which is larger than that for DNA, but as surface pretreatment neutralizes the mica surface, ns is significantly lowered. Equation 1 indicates that the concentration of monovalent counterions is considerably higher at the surface vicinity and decreases sharply within a few λ (Figure 1B). At short separation distances between DNA and mica, a strong entropic repulsion arises due to the compression of the mica and DNA clouds of counterions. More precisely, it occurs for distances of separation shorter than $d_{0(\mathrm{mica})} + d_{0(\mathrm{DNA})}$, where $d_{0(\mathrm{mica})}$ and $d_{0(\mathrm{DNA})}$ are the thicknesses of the mica and DNA counterion layers. These thicknesses are defined by the critical distance from the surfaces above which the counterions concentration equals the bulk cation concentration. In this respect, the thickness of the counterion layer depends on the salt concentration. For example, at 1 nm from the DNA surface, the DNA counterion concentration $n(d)$, is about 200 mM. Under high ionic strength (NaCl ≈ 200 mM), the increase of the total cation concentration due to the DNA surface is not very important at such a distance (2-fold). On the other hand, at the same distance and under lower ionic strengths (<30 mM), there is a huge increase of the total cation concentration (30 mM + 200 mM). As the entropic repulsion depends on the relative increase of the total cation concentration (bulk concentration + counterion concentration), a stronger and long-range repulsion is expected at low ionic strengths. Therefore a high monovalent salt concentration allows a closer approach of the DNA molecules to the surface, which should favor DNA binding on mica (Figure 1B). The critical separation distance below which DNA will interact electrostatically with the pretreated mica surface is about l_B, the Bjerrum length (0.7 nm at room temperature), l_B being the distance of separation from which the electrostatic potential of two elementary charges equals their thermal energy. We note in Figure 1B that the NaCl concentration should be larger than 200 mM to allow DNA adsorption on mica. We can also remark that neutralization of the mica by $NiCl_2$ pretreatment also leads to a slight increase of the range of the repulsion than for a bare mica. However this effect is counterbalanced by a lower entropic repulsion since the surface density of mica counterions decreases due to the mica surface neutralization by adsorbed Ni^{2+} ions during pretreatment.

(2) Origin of the DNA/Mica Attraction on $NiCl_2$ Pretreated Mica in Absence of Multivalent Cations. If DNA can approach the mica surface at other high ionic strengths, one question might then arise: What is the force that could then induce DNA adsorption? We know that nickel ions have a very high affinity for the mica surface as already demonstrated for many divalent transition metal cations.[39] Very strongly adsorbed nickel cations are thus not replaceable by monovalent ones.

In that context, a first explanation is a direct Columbic attraction between DNA phosphates and nickel ions. Since nickel cations have replaced potassium ions on mica, we can therefore expect that one nickel positive charge is still available for electrostatic attraction with negatively charged DNA phosphates. The potential overcharging of the $NiCl_2$ surface may help for DNA adsorption via a stronger electrostatic attraction. However, even thought the mica surface is positively charged or fully neutralized, the entropic repulsion overcomes the electrostatic attraction at low ionic strengths.[32,40] Therefore, a high ionic strength is still necessary to lower the entropic repulsion as for partially neutralized mica.

A second explanation is that the attraction is due to the counterion correlations between monovalent counterions on

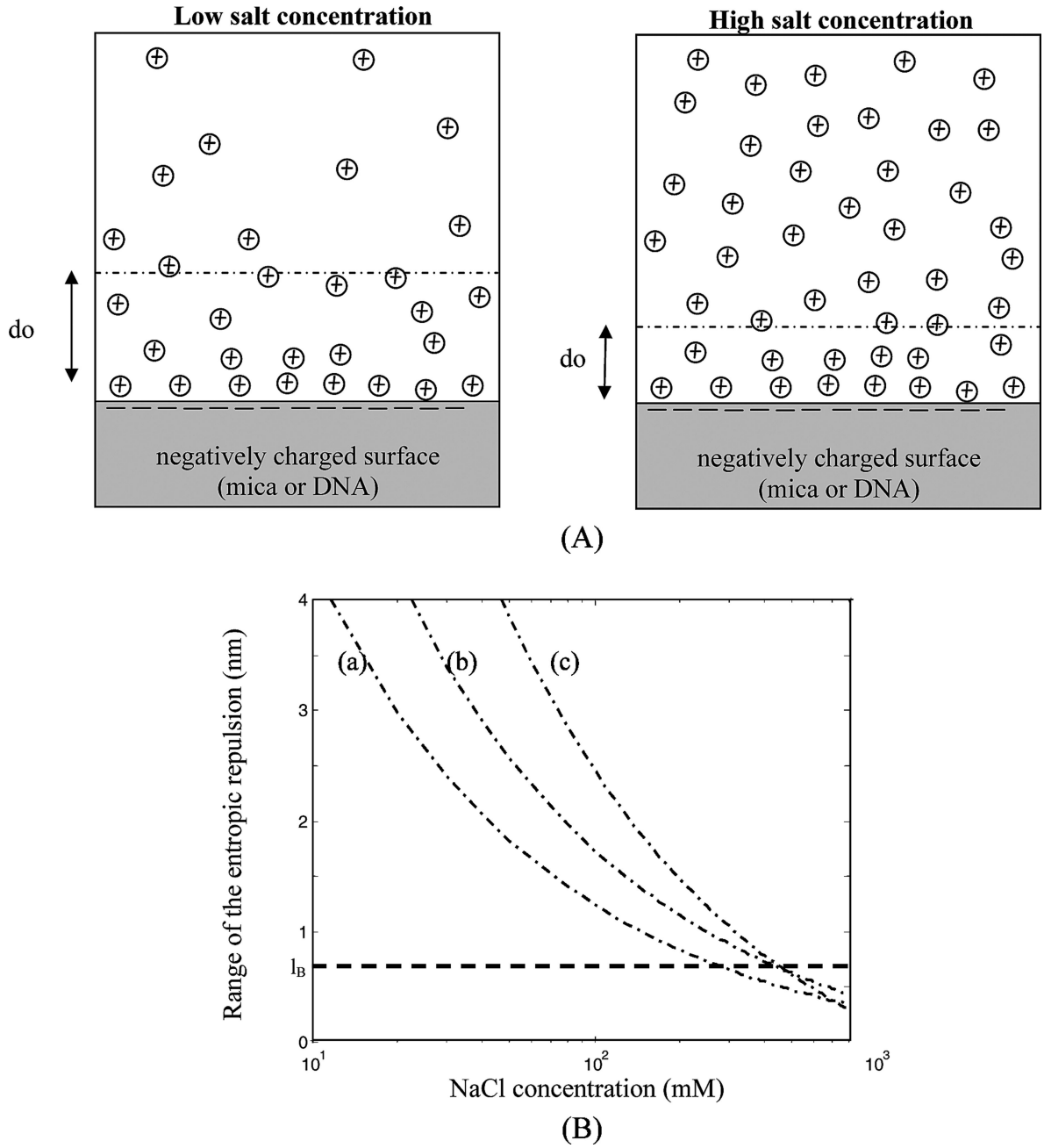

Figure 1. Model of DNA adsorption. (A) Schematic representation of the effect of increasing monovalent salt concentration on the thickness of the counterion layer for a negatively charged surface. d_0 is the distance at which the surface cation concentration is nearly equal to the bulk cation concentration. d_0 can be thought as the thickness of the cloud of counterions. It can be remarked that d_0 is reduced at high monovalent salt concentration (see the dotted lines). (B) Range of the repulsion force due to the compression of the mica and DNA counterion layers vs NaCl concentration for different mica surface charge densities: (a) bare mica, ns = 26 M; (b) partial neutralization (80%) by $NiCl_2$ pretreatment, ns = 5.3 M; (c) nearly fully neutralized mica surface by $NiCl_2$ pretreatment, ns = 1 M. l_B is roughly the critical distance separation required to bind DNA on a pretreated mica. Thus NaCl concentrations larger than 0.2 M needs to be used for DNA adsorption.

DNA surface and immobilized nickel ions on the mica surface. Counterion correlations between multivalent counterions were already demonstrated for DNA adsorption.[34] Concerning the correlations between monovalent DNA counterions and adsorbed nickel cations, the expected attraction should be weaker than that seen in the presence of multivalent cations and also independent of the ionic strength because nickel ions are not replaceable.

The last explanation is DNA/mica attraction mediated dispersion forces. It has been described that such force can arise for DNA molecules[41,42] or between DNA and mica[37] (van der Waals forces) and that the attraction is favored at high ionic strength.[37]

(3) Experimental Observation of DNA Adsorption on Mica at High Monovalent Salt Concentration. Figure 2 shows DNA molecules adsorbed on a 10 mM $NiCl_2$ pretreated mica surface at various NaCl concentrations. At low NaCl concentrations (<100 mM), DNA molecules were loosely adsorbed on the surface and appeared with globular shapes. When the monovalent salt concentration was increased (>10

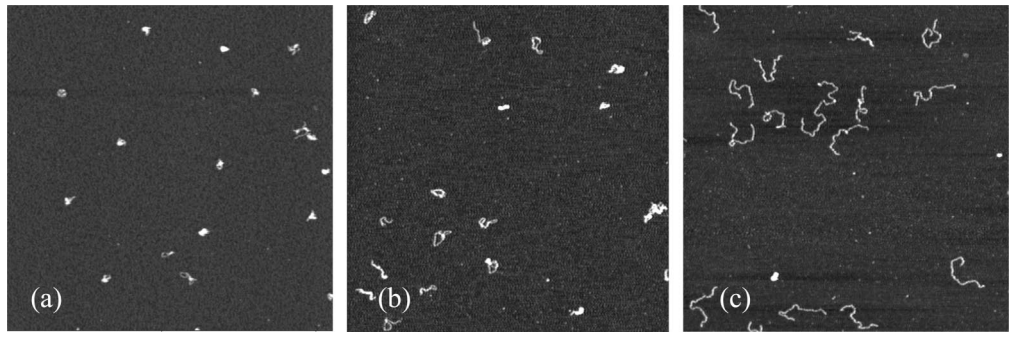

Figure 2. Effect of NaCl concentrations on 1440 bp DNA absorption on $NiCl_2$ pretreated mica in the presence of 20 mM Tris-HCl, pH 7.5, and (a) 50 mM NaCl, (b) 100 mM NaCl, and (c) 200 mM NaCl. DNA molecules were gradually adsorbed on the surface by increasing the monovalent salt concentration. Image area: 2.5 × 2.5 μm^2.

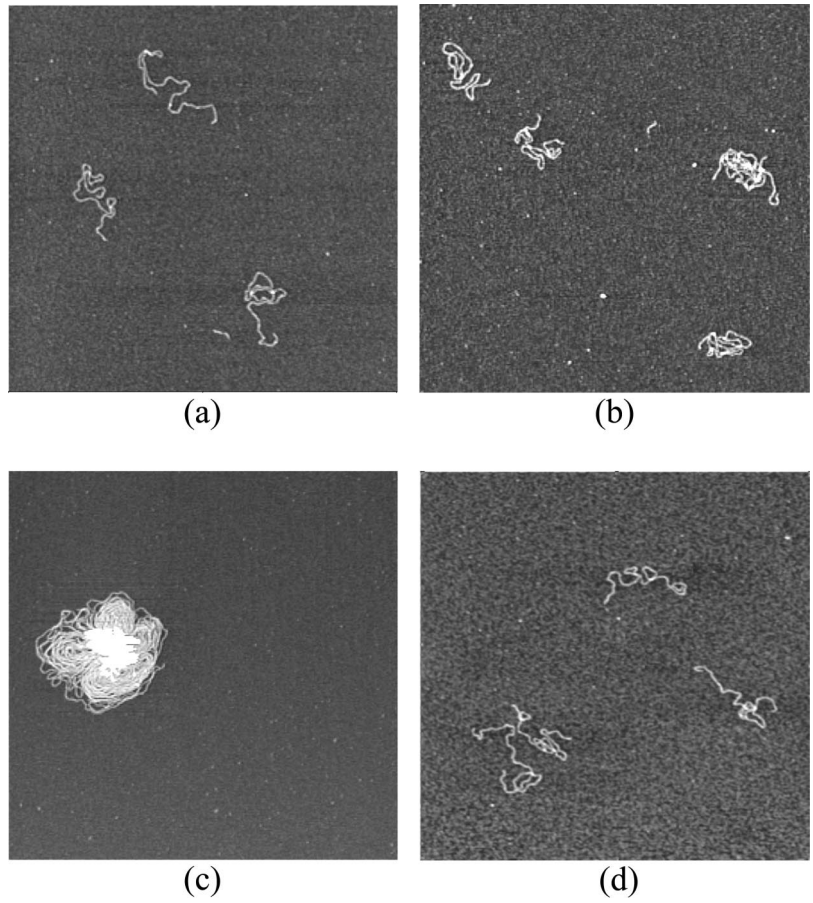

Figure 3. Gradual DNA compaction by macromolecular crowding. Linearized DNA plasmid (pBR322) was observed in presence of PEG of various molecular weights and at varying concentrations: (a) 10% (w/v) PEG 20K (50 mM NaCl, 20 mM Tris-HCl, pH 7.5), (b) 20% PEG 20K (50 mM NaCl, 20 mM Tris-HCl, pH 7.5), (c) 30% PEG 20K (50 mM NaCl, 20 mM Tris-HCl, pH 7.5), and (d) 30% PEG 1K (50 mM NaCl, 20 mM Tris-HCl, pH 7.5). DNA compaction was observed when the PEG 20K concentration was larger than 20% in 50 mM NaCl. PEG 1K did not induced DNA compaction, a result related to the small value of its gyration radius. It is also worth noting that a lower NaCl concentration is required to spread DNA on mica in the presence of PEG. Image area: 1.5 × 1.5 μm^2.

mM), we observed that the fraction of DNA molecules properly spread on the surface increased, which indicated a stronger adsorption in good agreement with the model that we developed (see Figure 1).

DNA Compaction under Macromolecular Crowding Conditions Observed by AFM

We then attempted to image DNA under conditions that mimic molecular crowding. Poly(ethylene glycol) (PEG) was chosen here as molecular crowding agent because of its wide use[5,6] and because it is a neutral polymer. Indeed, proteins such as bovine serum albumin are not appropriate due to their nonspecific binding on mica. Before AFM imaging, DNA molecules were spread in their conformation by rinsing the mica surface with 0.02% diluted uranyl acetate. There are some crucial advantages of using uranyl acetate prior to drying. First, uranyl acetate maintains previously adsorbed molecules on the surface during the drying step[34,43] and thus preserves the conformation adopted by the adsorbed molecules under macromolecular conditions. Second, uranyl acetate does not bind to neutral polymers and, thus, this step is also used to remove the PEG molecules, which would have perturbed AFM imaging. Dilution in water was not possible since a lower ionic strength induces DNA desorption (data not shown). Figure 3 shows the

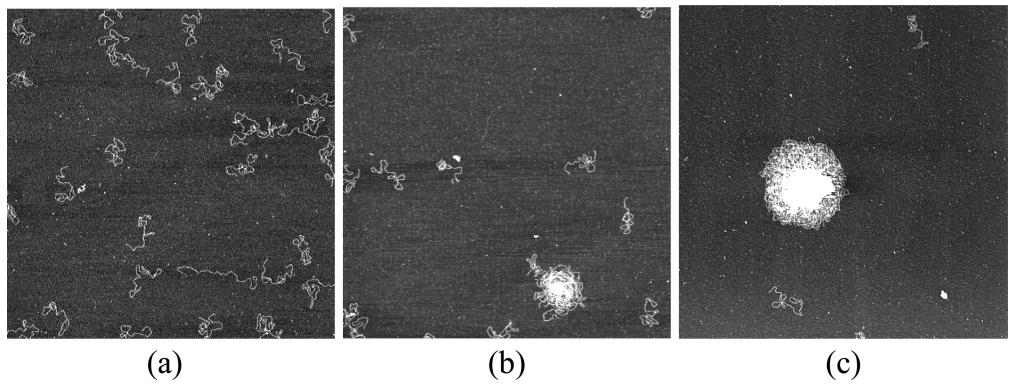

Figure 4. Influence of the PEG molecular weight on DNA compaction. Linearized pBR322 DNA (5μg/mL) was incubated for 5 min in 300 mM NaCl and 20 mM Tris-HCl, pH 7.5. Image areas: $3 \times 3\ \mu m^2$. (a) 10% PEG 1K (no compaction). (b) 10% PEG 4K. (c) 10% PEG 20K. Partial DNA compaction can be observed with PEG 4K and increase with PEG 20K. The size of the DNA aggregates and the compaction level seem to be higher with PEG 20K than with PEG 4K. It is worth noting that some isolated DNA molecules are not integrated within the big aggregates but they are less and less as the PEG molecular weight increases.

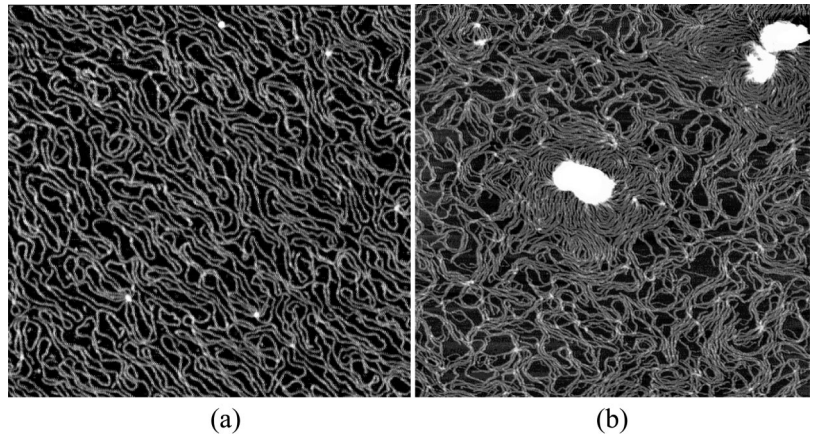

Figure 5. Image of DNA compaction. Linearized pBR322 DNA (15 μg/mL) was incubated for 5 min in 300 mM NaCl and 20 mM Tris-HCl, pH 7.5). (a) 15% PEG 1K (no compaction); (b) 15% PEG 20K. Image areas: $1.5 \times 1.5\ \mu m^2$.

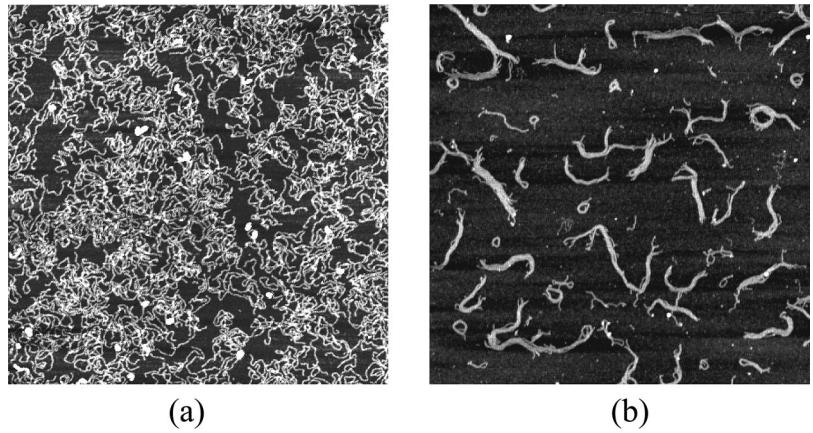

Figure 6. Surface bundling of adsorbed DNA molecules (1440 bp, 15 μg/mL) triggered by molecular crowding. (a) DNA molecules were adsorbed on $NiCl_2$-treated mica surface in a buffer solution containing divalent cations (50 mM NaCl, 10 mM $MgCl_2$, 20 mM Tris-HCl, pH 7.5). Then the sample was washed with buffer solution to remove unbound DNA molecules. (b) Image of the adsorbed DNA molecules after 5 min of incubation in a PEG 20K solution (300 mM NaCl, 20% (w/v) PEG 20K, 20 mM Tris-HCl, pH 7.5). The combination of molecular crowding and high ionic strength led to the formation of DNA bundles on the surface. Image areas: $2.5 \times 2.5\ \mu m^2$.

DNA conformational changes of linear DNA fragments as a function of PEG 20K concentrations in 20 mM Tris pH 7.5, 50 mM NaCl. At 10% (w/v) PEG 20K, adsorbed DNA molecules were extended on the surface but, as the PEG concentration increased, compaction of the DNA molecules and (or) an association between DNA molecules was observed (see Figure 3b). For PEG 20K concentrations larger than 20%, DNA condensation was triggered and DNA aggregates were observed on the surface (see Figure 3c). Figure 3d shows that PEG 1K cannot induce DNA compaction as expected due to its small radius of gyration, which scales like $MW^{3/5}$ (MW being the PEG molecular weight). Indeed it is generally known that macromolecular crowding induces a depletion attraction due to excluded volume interactions between DNA molecules.[18,44] We also tested that the critical PEG concentration required to trigger DNA compaction can be lowered by increasing NaCl concentration, which is a well-known characteristic

of the DNA compaction by depletion attraction due to macromolecular crowding.[18,45] These results clearly indicate that DNA compaction was triggered by macromolecular crowding in the presence of only monovalent salt and PEG molecules.[46]

In Figure 4, we observed on larger areas the attraction between DNA molecules mediated by macromolecular crowding in the presence of PEG for different molecular weights. With PEG 4K and PEG 20K, multimolecular aggregation of DNA molecules was observed. In addition, the size and the level of DNA compaction increased with the molecular weight. Isolated DNA molecules, which were not incorporated within the DNA aggregates, were observed and appeared in a relaxed form. Monomolecular compaction should also have been observed under such conditions (10% PEG 20K, 300 mM NaCl) but the spreading of the isolated molecules on the surface, as it was observed for DNA compaction mediated by polyamines,[34,46] could induce a more relaxed appearance.

DNA adsorption on a $NiCl_2$ pretreated mica in the presence of monovalent salt appeared thus unique in its capacity to observe DNA by AFM at physiological ionic strength and under crowded environments making it possible to observe DNA compaction[12,17] at a nanometer scale. For example, Figure 5 represents linearized pBR322 DNA molecules at high ionic strength (300 mM NaCl) which were compacted in bulk solution under excluded-volume conditions (15% (w/v) PEG 20K). This figure shows the formation of large DNA aggregates. The compaction of DNA molecules, which were previously adsorbed on the surface, was also investigated using our method as represented in Figure 6. A high concentration (15 μg/mL) of 1440 bp linear DNA molecules was used to obtain a high coverage of the mica surface with DNA. The sample was then washed with buffer to remove molecules not adsorbed on the surface. Then, a PEG solution (20% PEG 20K, 300 mM NaCl) was added to trigger DNA condensation on the surface. The combination of high salt concentration and high concentration of PEG 20K led to DNA interassociation on the surface. The mean height of DNA structures presented in Figure 6b was 2 nm, which clearly indicated that they were composed of only one layer of DNA molecules. So, molecular crowding leads to DNA bundling on the surface. Large globules and toroids can be also observed but to a less extent. The diameter of the smallest toroids was around 50 nm, which is about the DNA persistence length, and may involve single DNA molecule. Monomolecular condensation of previously adsorbed DNA can thus be observed under macromolecular crowding conditions by using a high PEG 20K concentration to limit the spreading effect of the surface.

In conclusion, we have demonstrated here that imaging DNA by AFM can be performed in presence of high monovalent salt concentration and high molecular weight PEG. This strategy opens new perspectives to explore the influence of macromolecular crowding on DNA conformation and DNA–protein processes (transcription, replication, repair) at the nanometer scale and to help the design of DNA-inspired applications (DNA self-assembly).

Acknowledgment. This work was supported by the Association pour la Recherche sur le Cancer (ARC).

Supporting Information Available. Image showing the formation of DNA bundles on a mica surface. This material is available free of charge via the Internet at http://pubs.acs.org.

References and Notes

(1) Zimmerman, S. B.; Minton, A. P. *Annu. Rev. Biophys. Biomol. Struct.* **1993**, *22*, 27–65.
(2) Minton, A. P. *J. Biol. Chem.* **2001**, *276*, 10577–10580.
(3) Ellis, R. J. *Trends Biochem. Sci.* **2001**, *26*, 597–604.
(4) Rivas, G.; Ferrone, F.; Herzfeld, J. *EMBO Rep.* **2004**, *5*, 23–27.
(5) Zimmerman, S. B.; Harrison, B. *Proc. Natl. Acad. Sci. U.S.A.* **1987**, *84*, 1871–1875.
(6) Naimushin, A. N.; Quach, N.; Fujimoto, B. S.; Schurr, J. M. *Biopolymers* **2001**, *58*, 204–217.
(7) Ellis, R. J.; Minton, A. P. *Nature* **2003**, *425*, 27–28.
(8) Terry, B. J.; Jack, W. E.; Rubin, R. A.; Modrich, P. *J. Biol. Chem.* **1983**, *258*, 9820–9825.
(9) von Hippel, P. H.; Berg, O. G. *J. Biol. Chem.* **1989**, *264*, 675–678.
(10) Parsegian, V. A.; Rand, R. P.; Rau, D. C. *Proc. Natl. Acad. Sci. U.S.A.* **2000**, *97*, 3987–3992.
(11) Mel'nikov, S. M.; Khan, M. O.; Lindman, B.; Jonsson, B. *J. Am. Chem. Soc.* **1999**, *121*, 1130–1136.
(12) Cunha, S.; Woldringh, C. L.; Odijk, T. *J. Struct. Biol.* **2001**, *136*, 53–66.
(13) Louie, D.; Serwer, P. *J. Mol. Biol.* **1994**, *242*, 547–558.
(14) Erijman, L.; Clegg, R. M. *Biophys. J.* **1998**, *75*, 543–462.
(15) Sanders, G. M.; Kassavetis, G. A.; Geiduschek, E. P. *Proc Natl. Acad. Sci. U.S.A.* **1994**, *91*, 7703–7707.
(16) Goobes, R.; Cohen, O.; Minsky, A. *Nucleic Acids Res.* **2002**, *30*, 2154–2161.
(17) Zimmerman, S. B.; Murphy, L. D. *FEBS Lett.* **1996**, *390*, 245–248.
(18) Kleideiter, G.; Nordmeiner, E. *Polymer* **1999**, *40*, 4013–4023.
(19) Katsura, S.; Hirano, K.; Matsuzawa, Y.; Yoshikawa, K.; Mizuno, A. *Nucleic Acids Res.* **1998**, *26*, 4943–4945.
(20) Veaute, X.; Jeusset, J.; Soustelle, C.; Kowalczykowski, S. C.; Le Cam, E.; Fabre, F. *Nature* **2003**, *423*, 309–312.
(21) Frenkiel-Krispin, D.; Levin-Zaidman, S.; Shimoni, E.; Wolf, S. G.; Wachtel, E. J.; Arad, T.; Finkel, S. E.; Kolter, R.; Minsky, A. *EMBO J.* **2001**, *20*, 1184–1191.
(22) Hud, N. V. *Biophys. J.* **1995**, *69*, 1355–1362.
(23) Murphy, L. D.; Zimmerman, S. B. *J. Struct. Biol.* **1997**, *119*, 336–346.
(24) Mangenot, S.; Leforestier, A.; Durand, D.; Livolant, F. *J. Mol. Biol.* **2003**, *333*, 907–916.
(25) Thundat, T.; Allison, D. P.; Warmack, R. J.; Brown, G. M.; Jacobson, K. B.; Schrick, J. J.; Ferrell, T. L. *Scanning Microsc.* **1992**, *6*, 911–918.
(26) Thomson, N. H.; Kasas, S.; Smith, B. L.; Hansma, H. G.; Hansma, P. K. *Langmuir* **1996**, *12*, 5905–5908.
(27) Piétrement, O.; Pastré, D.; Fusil, S.; Jeusset, J.; David, M.-O.; Landousy, F.; Hamon, L.; Zozime, A.; Le Cam, E. *Langmuir* **2003**, *19*, 2536–2539.
(28) Bezanilla, M.; Drake, B.; Nudler, E.; Kashlev, M.; Hansma, P. K.; Hansma, H. G. *Biophys. J.* **1994**, *67*, 2454–2459.
(29) Hegner, M.; Wagner, P.; Semenza, G. *FEBS Lett.* **1993**, *336*, 452–456.
(30) Mou, J.; Czajkowsky, D. M.; Zhang, Y.; Shao, Z. *FEBS Lett.* **1995**, *371*, 279–282.
(31) Hansma, H. G. *Annu. Rev. Phys. Chem.* **2001**, *52*, 71–92.
(32) Pastré, D.; Piétrement, O.; Fusil, S.; Landousy, F.; Jeusset, J.; David, M. O.; Hamon, L.; Le Cam, E.; Zozime, A. *Biophys. J.* **2003**, *85*, 2507–2518.
(33) van Noort, S. J.; van der Werf, K. O.; Eker, A. P.; Wyman, C.; de Grooth, B. G.; van Hulst, N. F.; Greve, J. *Biophys. J.* **1998**, *74*, 2840–2849.
(34) Pastré, D.; Hamon, L.; Landousy, F.; Sorel, I.; David, M. O.; Zozime, A.; Le Cam, E.; Pietrement, O. *Langmuir* **2006**, *22*, 6651–6660.
(35) Fang, Y.; Hoh, J. H. *Nucl. Acids. Res.* **1998**, *26*, 588–593.
(36) Ellis, J. S.; Abdelhady, H. G.; Allen, S.; Davies, M. C.; Roberts, C. J.; Tendlers, S. J. B.; Willams, P. M. *J. Microsc.* **2004**, *215*, 297–301.
(37) Sushko, M. L.; Shluger, A. L.; Rivetti, C. *Langmuir* **2006**, *22*, 7678–7688.
(38) Rouzina, I.; Bloomfield, V. A. *J. Phys. Chem.* **1996**, *100*, 4292–4304.
(39) Hansma, H. G.; Laney, D. E. *Biophys. J.* **1996**, *70*, 1933–1939.
(40) Lau, A. W. C.; Pincus, P. *Eur. Phys. J. B* **1999**, *10*, 175–180.
(41) Bloomfield, V. A.; Wilson, R. W.; Rau, D. C. *Biophys. Chem.* **1980**, *11*, 339–343.
(42) Sottas, P. E.; Larquet, E.; Stasiak, A.; Dubochet, J. *Biophys. J.* **1999**, *77*, 1858–1870.
(43) Pastré, D.; Piétrement, O.; Zozime, A.; Le Cam, E. *Biopolymers* **2005**, *77*, 53–62.
(44) de Vries, R. *Biophys. J.* **2001**, *80*, 1186–1194.
(45) Zinchenko, A. A.; Yoshikawa, K. *Biophys. J.* **2005**, *88*, 4118–4123.
(46) Besteman, K.; Vilfan, K. v. E.; Vilfan, I. D.; Ziese, U. Lemay, S. G. *Biopolymers*.

BM700856U